ORIGINAL ARTICLE

Comparative PGA-driven probabilistic seismic hazard assessment (PSHA) of Turkey with a Bayesian perspective

Murat Nas (ORCID) · **Alexey Lyubushin** · **Mustafa Softa** ·
Yusuf Bayrak

Abstract While there has been significant research on probabilistic seismic hazard analysis (PSHA) using several different seismic sources, this paper focuses particularly on understanding the spatially varying seismic hazard controlled only by earthquakes. In that vein, regarding Turkish seismicity, this study is the first of its kind to explore this conundrum from a Bayesian point of view and offer new estimates to compare with the existing ones. In this study, a national-extent peak ground acceleration (PGA)–driven hazard map (upon 90% quantile of maxima, $V_{S30} = 760$ m/s, and a return period of 475 years) was created and then compared both with the old and new versions of the officially recognized seismic hazard maps of Turkey. Regarding 10 earthquake-prone cities, the new PGA estimates were compared with those picked from these two maps. Next, individual site-based hazard estimates were drawn for these city centers considering the return periods of 43, 72, 140, and 475 years. The present hazard map was in compliance with the seismotectonic setup of Turkey and its PGA estimates were slightly high compared with the last two hazard maps for some specific regions, most of which are located in major active fault zones with a history of intense seismic activity, albeit the figures for low seismic zones were relatively low. With this study, it becomes clear that the process of PSHA, which innately requires a long and tiresome effort, can instantaneously be performed against the changing of catalog data over time, and thence prompt evaluations on variations can consequently be made.

Keywords Probabilistic seismic hazard analysis (PSHA) · Peak ground acceleration (PGA) · Seismicity of Turkey · Bayesian estimation · Posteriori probability

M. Nas (✉)
Department of Civil Engineering, Karadeniz Technical University, 61080 Trabzon, Turkey
e-mail: muratnas@ktu.edu.tr

A. Lyubushin
Institute of Physics of the Earth, Russian Academy of Sciences, Bolshaya Gruzinskaya, 10, Moscow, Russia

M. Softa
Department of Geological Engineering, Dokuz Eylül University, 35390 Izmir, Turkey

Y. Bayrak
Department of Geophysics, Karadeniz Technical University, 61080 Trabzon, Turkey

1 Introduction

One of the most significant aspects of seismicity is its spatiotemporally varying and mostly implicit potential for creating instantaneous structural damage. Among several strong ground-motion amplitudes, the horizontal component of peak ground acceleration (PGA) has widely been used for both structural vulnerability assessment and design of earthquake-resistant structures. Therefore, a significant fraction of seismic hazard assessments is carried out with a focus on PGA. The aim of seismic hazard analysis, done by purpose-oriented statistical methodologies mostly based on the contents of known parameters, is to determine the annual

frequency of exceedance or rather the annual frequency of non-exceedance belonging to specific amplitude, having specific intensity, considering a given future time interval. Contrary to frequency-based statistics, the Bayesian perspective aims to define the probability of an occurrence based on a priori information on the pertinent states relating to the primary phenomena. Besides, the Bayesian probability theory supplies several flashing opportunities and versatile tools for estimating characteristic seismicity parameters that can easily be used to determine seismic hazard potential. The Bayesian perspective is rather based on a posterior belief. In this sense, one of the genuine advantages of Bayesian approaches is that it provides users with an excellent opportunity to take into account the uncertainty of each parameter used in probabilistic relationships as well as a priori knowledge (Campbell 1982; Campbell 1983; Galanis et al. 2002; Kelly and Smith 2011; Mortgat and Shah 1979).

In the present paper, we implemented a Bayesian methodology, which was first postulated by Pisarenko et al. (1996) and then improved and generalized by Pisarenko and Lyubushin (1997) and Pisarenko and Lyubushin (1999), in order to illuminate the PGA-driven seismic hazard of Turkey. The focus of the paper is on the delineation of one of the most essential seismic hazard parameters, namely the expected maximum values of PGA and quantiles of the pertinent probabilistic distributions taken into account for the given future intervals for the whole mainland of Turkey.

In a very short history, the first attempt to use the method of Pisarenko et al. (1996) in zone-based hazard analysis, or in other words grid-based computations, which is similar but far beyond the single-site-based analysis, was given by Lyubushin and Parvez (2010). Later on, another example was recently done by Salahshoor et al. (2018) for Iran. To the best of our knowledge, on the one hand, no further implementation of the same methodology has as yet been done for any other place. On the other hand, using Pisarenko et al. (1996), several site-based analyses were conducted to estimate seismic hazard parameters in multifarious regions of the world to date. These implementations conducted to date can be classified into three different categories, to wit (i) the maximum possible magnitude estimations (M) and its related statistical parameters (β, λ) (Bayrak and Türker 2016; Bayrak and Türker 2017; Mohammadi et al. 2016; Pisarenko and Lyubushin 1999; Pisarenko et al. 1996; Ruzhich et al. 1998;

Tsapanos 2003; Tsapanos and Christova 2003; Tsapanos et al. 2001; Yadav et al. 2013a), (ii) peak ground acceleration (PGA or A_{max}) (Lyubushin and Parvez 2010; Lyubushin et al. 2002; Pisarenko and Lyubushin 1997), and (iii) tsunami intensity (I) (Yadav et al. 2013b).

The present paper focuses on delineating the maximum horizontal peak ground acceleration (PGA) estimates for Turkey using an updated earthquake catalog and the Bayesian methodology aforementioned. Of several outputs of this study, the new national PGA hazard map got prepared. Besides, various return periods were used in several site-based analyses. After having performed consecutive analyses, through available information and GIS tools, we compared some outputs of this study with the last two official seismic hazard maps (upon 475-year return period) of Turkey. Of two maps, the predecessor hazard map is known to be one of the several results of the study made by Gülkan et al. (1993) (hereafter referred to as G93). G93 was created in the form of a zonation map, which has long been known as a long-sought-after mapping concept in earthquake engineering practices. Having said that, the successor hazard map (AFAD 2018) is a core part of the results of the comprehensive study officially entitled "the revised national probabilistic seismic hazard maps project" (hereafter T-SHM project). Some components of the T-SHM project (Akkar et al. 2018b; Demircioğlu et al. 2018; Duman et al. 2018; Emre et al. 2018; Eroglu Azak et al. 2017; Kadirioğlu et al. 2016; Şeşetyan et al. 2018) are now available in the literature. In addition to map-based comparisons, we further compared the new hazard estimates belonging to ten earthquake-prone cities with those figures taken from the last two national seismic hazard maps of Turkey.

2 Brief seismotectonic setup of Turkey

Turkey has actively been undergoing an explicit deformation as a result of the characteristically distinguishable continental collision between the plates of Africa, Arabia, and Eurasia, which is even originated from the Mesozoic split-up of Gondwana. Because of that, Turkey is thenceforth known to be one of the extraordinarily active regions of the world in terms of seismic activity (Harrison 2008; Jackson 1994; Şengör et al. 1984). Due to particular deployment in the Alpine Himalayan orogenic belt, a great variety of evolutionary geologic

structures and destructive seismic events originate from the active neotectonics of Turkey. Highly seismically active Anatolian plate has been moving obliquely since the Miocene. The movement is suggested to be related both to subduction processes that take place in the Aegean–Cyprus Arc (AA-CA) and to the explicit collision between Arabia and Eurasia (Royden 1993; Şengör et al. 1984). The convergence between the Eurasian and Arabian plates creates immense coercion into the plate boundaries, which specifically makes each part of the country an emblematic area of the modern global seismology.

The main neotectonic structures of Turkey, which are of great potential to produce consecutive destructive earthquakes, are briefly categorized into significant major zones, namely North Anatolian Fault Zone (NAFZ), East Anatolian Fault Zone (EAFZ), Dead Sea Fault Zone (DSFZ), and Aegean–Cyprus Arc (Bozkurt 2001). These fault zones are thought to have inherited from the structures that were active even before Miocene time (Yılmaz et al. 1997). Tectonic evidence-based judgments of McKenzie (1972) denote and broadly justify that the Anatolian plate is in a relative westward movement to the Eurasian plate. Since the Eurasian plate is pretending to be stable, the ongoing convergence of Arabian and African plates, which is in northward movement, creates the most seismically active transform zones of the Earth called North Anatolian Fault Zone (NAFZ). One of the main characteristics of North Anatolian Fault (NAF) is that it delineates the transform plate boundary between the Anatolian and Eurasian plates, which extends for a length of 1200 km (Şengör et al. 2005). It is mostly interpreted by making some sort of affinity-based simulations with the San Andreas Fault of California (Allen 1982). In point of fact, each of them is in dextral strike-slip motion generating large-scale crustal deformations, and thus large earthquakes (Hussain et al. 2018; McClusky et al. 2000; Reilinger et al. 2006; Reilinger et al. 1997; Şengör et al. 2005). In addition, NAFZ is of multiple synthetic and antithetic faults just like the Northeastern Anatolian Fault Zone (NEAFZ) (Badgley 1965; Vialon et al. 1976; Wilcox et al. 1973). NEAFZ, which is about 800 km in length, is a northeasterly trending dextral strike-slip fault. It has a north-dipping thrust fault, which is about 250-km length (Koçyiğit et al. 2001; Westaway 1994). Besides, the connection between NEAFZ and NAF gets integrated by 400-km-long northeast-trending and south-dipping Black Sea Fault (BSF),

which has a ramp-flat structure depicted in Fig. 1 (Softa et al. 2018; Softa et al. 2019). As is well known from past events, most of the major large earthquakes occurred at the nodes of these active structures and they should again be expected to happen thereabout (Tuyen and Lu 2012).

Principally, the seismic activity of the Eastern Anatolian region originates from the amalgamated convergence of the Eurasian, African, and Arabian plates that exposes the region to explicit northward motion (Dewey et al. 1986; McKenzie 1976). The zone of Aegean–Cyprian Arc, which is of a great potential to produce rather deep earthquakes, shows specific tectonic characteristics that stemmed from plunging motion into the oceanic lithosphere beneath the Anatolian plate due to the northward motion of the African plate (Jackson 1994; Pichon and Kreemer 2010; Reilinger et al. 2006) (for in-depth review and discussions, we recommend readers to examine the following resources: Barka 1992; Delph et al. 2015; Duman and Emre 2013; Saroglu et al. 1992; Şengör et al. 1985; Şengör and Yilmaz 1981; Tatar et al. 2013; Turkelli et al. 2003). An illustrative map explaining the brief amalgamated geologic and tectonic map of the Anatolia–Caucasus region is set out in Fig. 1 and the map of the brief seismotectonic setup of Turkey with the earthquake occurrences experienced in the last 118-year is given in Fig. 2.

3 Data and resources used

The first and the foremost input of the Bayesian method (Pisarenko et al. 1996) is the spatial data of seismicity for a given enclosed region; namely, it is the earthquake catalog of Turkey. For Turkey and adjacent areas, aside from the old ones, recently compiled different instrumental earthquake catalogs (Akkar et al. 2010; Duman et al. 2016; Kadirioğlu et al. 2016; Kalafat et al. 2011; Leptokaropoulos et al. 2013) were published for several purposes by various researchers to date. In addition, several studies partially or totally covering Turkey (Ambraseys and Jackson 2000; Guidoboni et al. 1994; Shebalin et al. 1998; Soysal et al. 1981; Stucchi et al. 2013; Tan et al. 2008) were conducted to compile and merge the historical earthquakes that happened before the instrumental era of seismology.

Of all the available catalogs, Kadirioğlu et al. (2016) recently published one of the sound examples of the unified earthquake (1900 to 2012) catalogs
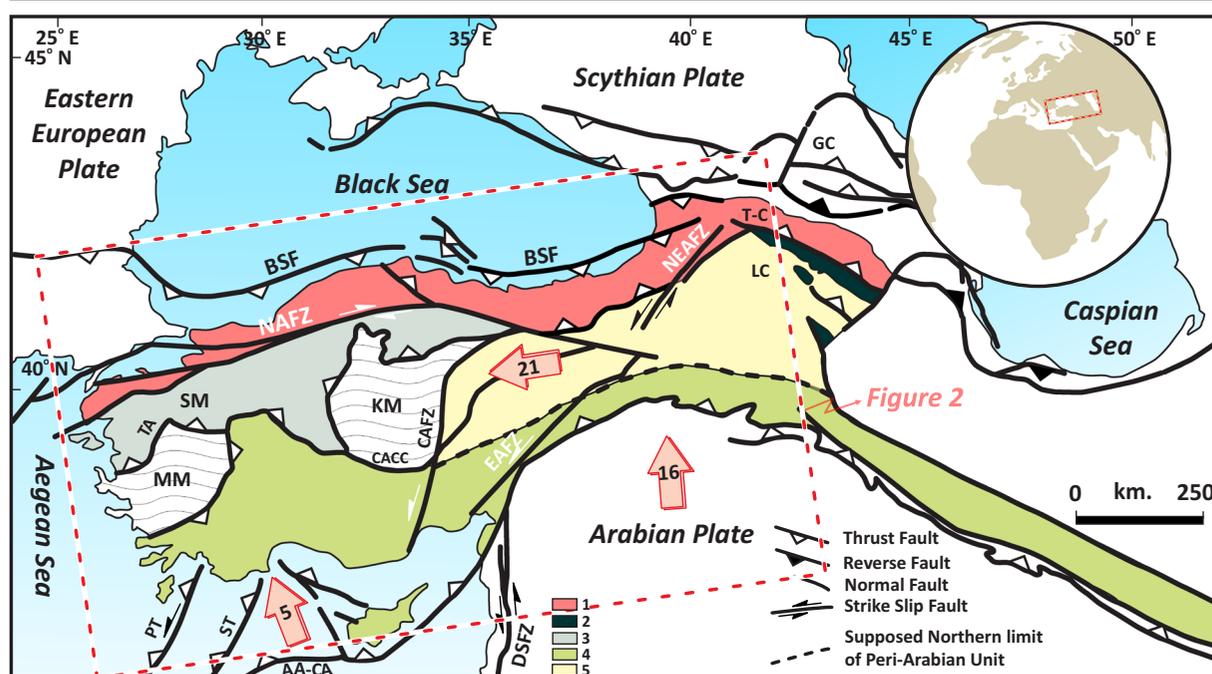
Fig. 1 Brief amalgamated geologic and tectonic map of the Anatolia–Caucasus region, after Sosson et al. (2016) and Hässig et al. (2016) with modifications. NAFZ, North Anatolian Fault Zone; CAFZ, Central Anatolian Fault Zone; EAFZ, East Anatolian Fault Zone; NEAFZ, Northeast Anatolian Fault Zone; BSF, Black Sea Fault; DSFZ, Dead Sea Fault Zone; PT, Plino Trench; ST, Strabo Trench; AA-CP, Aegean–Cyprus Arc; GC, Greater Caucasus; LC, Lesser Caucasus; T-C, Trans Caucasus; KM, Kirsehir Massif; MM, Menderes Massif; SM, Sakarya Massif; CACC, Central Anatolian Crystalline Complex; EAP, East Anatolian Block; R-K, Rioni Kura Basin; TA, Tavsanli and Afyon Zones. 1, European margin including magmatic arc; Pontides/Somkheto-Karabakh; 2, Ophiolites; 3, Sakarya accreted terrane; 4, Peri-Arabic units (Lycian nappes); 5, Taurides–Anatolides, East Anatolian accreted terrane. Solid yellow arrows with numbers represent plate movement (mm a^{-1}) with respect to a stable Eurasia (Reilinger et al. 2006)

homogenized into a moment magnitude scale (Mw) ever created for Turkey. This catalog is not only the core catalog of the present study, which was particularly updated for our hazard assessments, but also it is the same catalog with that used in the T-SHM project. Initially, we updated the core catalog at the outset. To this end, two online and officially published earthquake databases (#1 KOERI, http://udim.koeri.boun.edu.tr/zeqdb/, last accessed on 07 March 2018; #2 TR-NSMN, http://kyhdata.deprem.gov.tr/2K/kyhdata_v4.php, last accessed on 07 March 2018) were used to collect further events to make the core catalog update. The further events were selected from those events that occurred between 25 December 2012 and 07 March 2018. Before merging two datasets (core and further) into a single catalog, it was necessary to bring further data to the same scale as the core one. To homogenize the further events, moment magnitude-oriented conversion relations provided by Kadirioğlu and Kartal (2016) were then used when necessary as fully in line with the methodology adopted in Kadirioğlu et al. (2016).

In the meantime, no historical event that occurred before the year 1900 was added to the catalog. The primary reason for this preference is that the method used in this paper requires a continuous catalog so that it can statistically be handled. Namely, the catalog must not be of incomplete data; otherwise, the results of the Bayesian perspective might shift from what exactly could be. The specific example of this fact was showed in a comparative hazard study recently conducted by Salahshoor et al. (2018) for Iran. The spatial distribution of the fully merged catalog (hereafter catalog) over Turkey is shown in Fig. 2. The catalog comprises 13,564 events in total being dependents and independents events altogether.

Besides, to estimate PGA values upon a given future period, all data were retested for the responsiveness level of the method postulated by Pisarenko et al. (1996). As with the seismic hazard analysis pathway,
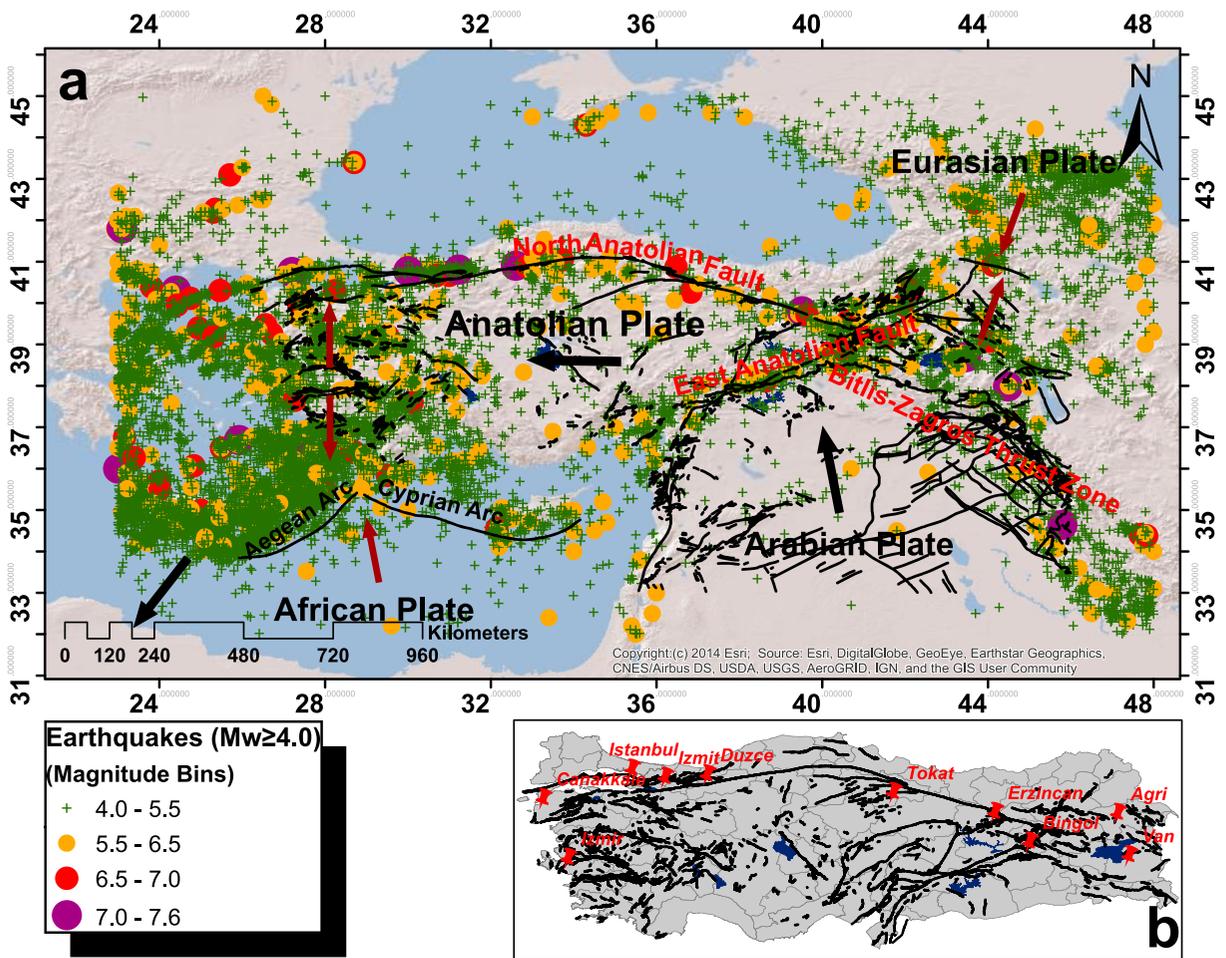
Fig. 2 **a** Illustrative map of the brief seismotectonic setup with earthquakes occurred between 1900 and 2018 in and around Turkey used in this study. **b** Site location map of the surveyed ten earthquake-prone cities of Turkey in this study

the adopted methodology requires mounting the proper ground-motion prediction equations (GMPEs) to the logic tree to be used as a second input to the method, and then all of which are submitted to the compound hazard integral. It is crucial to any seismic hazard analysis for which GMPEs are to be used. No matter which GMPEs are used, the raising epistemic uncertainty is inevitable. Epistemic uncertainty is a disruptor factor that increases the potential bias in seismic hazard analyses (Bommer 2012; Scherbaum et al. 2005; Scherbaum and Kuehn 2011).

As is stated by Kale and Akkar (2013), of several goodness-of-fit measures, the most prevalent way of testing and ranking the GMPEs depending on their performance is the residual-driven methods. In that respect, several ranking and selection techniques have so far been developed and used. Even though it was

particularly designed for different scientific disciplines, the concept of the Nash–Sutcliffe efficiency (NSE) coefficient (Nash and Sutcliffe 1970) and its modified way of implementation (McCuen et al. 2006) are used as a tool of goodness-of-fit measure for analyzing the GMPEs. Scherbaum et al. (2004) developed a new goodness-of-fit measure based on the concept of likelihood, LH, and Scherbaum et al. (2009) designed a log-likelihood differences technique, LLH. With an effective and progressive perspective, Yaghmaei-Sabegh (2012) put forward to an alternative and rather advanced technique for ranking and weighting of GMPEs based on artificial neural networks (ANN). Kale and Akkar (2013) developed a new approach called the Euclidean distance-based ranking (EDR) method. In this study, regarding specifying and weighting GMPEs to be used in the logic tree, we adopted the results of Akkar et al.

(2018b) used in the computations of the recent earthquake hazard map of Turkey (AFAD 2018). The main reason for this is that the earthquake catalog used in the present study is diametrically the same as the one used in the T-SHM project, except for the addition of earthquake data concerning the preceding few years to update it. In the T-SHM project, Akkar et al. (2018b) first selected a bunch of relations from several national and global GMPEs as candidate models and all models were then assessed by data-driven testing techniques not only for delineating which models are the best result-giving ones according to earthquake database but also for what the sound weight must be assigned to each model. After having tested several GMPEs, in consequence, they decided to mount the selected successful ground-motion models to the complete hazard model. As is mentioned above, the body of the seismic source model of the T-SHM project is attributed to three kinds of sources; howbeit, the ground-motion models were divided into two categories. On the one hand, the first group is for the representations of the shallow crustal seismicity modeled with the GMPEs of Akkar et al. (2014) (hereafter referred to as AK14), Akkar and Çağnan (2010) (hereafter AC10), and Chiou and Youngs (2008) (hereafter CY08) by assigning a weight of 1/3 to each relation. On the other hand, the second group that epitomizes the subduction and interface zones is modeled by GMPE models of Megawati and Pan (2010) for interface regions and through the model of García et al. (2005) for in-slab regions with an individually unique weight of 1.0. Because the focus of the paper is not only on the generation of national seismic hazard map of Turkey but also on ensuring affinity between the past two studies to the extent possible, the GMPEs used in the T-SHM project for the shallow crustal seismicity of Turkey were adopted verbatim in our modeling phase.

Of several distance metrics, epicentral distance and Joyner–Boore distance (Joyner and Boore 1981) (hereafter JB distance) genuinely dominate the realm of the GMPEs. When using different metrics at the same time, a distance adjustment, which inevitably creates a somewhat escalation in the aleatory uncertainty of the hazard model, is crucially required to stabilize the distance metrics. To that end, the Electric Power Research Institute (EPRI 2004) suggested a series of distance conversion pathways depending on several modeling assumptions with respect to the epicenter location of an earthquake relative to the fault rupture. The modeling is done

through either random epicenters approach, which is based on the assumption that the epicenter of an earthquake is uniformly distributed along the full length of the rupture or hypothetically centered epicenters, which is based on the assumption that the epicenter of an earthquake is expressly centered on the earthquake rupture. In the present study, now that the adopted ground-motion model of the logic tree is of three components and a great majority of which use the JB distance, we used the JB distance of each earthquake. This expedient is useful both for the homogenization of the distances and for tamping down the total amount of aleatory uncertainty to the highest possible extent. To this end, we adopted the random epicenter model of EPRI (2004) for the distance adjustments on the grounds that it is thought to be more consistent with the perplexing and amalgamated seismotectonic setup of Turkey as briefly explained above.

Besides, as is well known, local site conditions of the ground-motion recording sites profoundly affect the measured PGA values. Each GMPE that we used in this study includes a V_{S30} term, and it inevitably makes the result of PGA calculations (the spectral period is zero) site-dependent. In this perspective, the PGA values got computed by taking into account the reference-rock site condition for $V_{S30} = 760$ m/s seeing that this value was applicable to all GMPEs used in the present study, and it denotes B/C boundary value in keeping with the classification of National Earthquake Hazards Program of the USA (NEHRP) (BSSC 2001). Furthermore, the results obtained through the fixed V_{S30} approach provided a great convenience in that it made our results comparable with the outcomes of the successor and predecessor hazard maps of Turkey.

Upon the completion of the T-SHM project, the hazard map and its index list were given in an annex to a decree in a form of read-only PDF file, https://deprem.afad.gov.tr/images/depbolge/deprem-tehlike-haritasi.pdf, last accessed on 01 May 2020. We used the official seismic hazard map of Turkey (AFAD 2018) in our comparative calculations whereupon we created a digital map upon retyping the pertinent parts of this rather long document. Furthermore, using coordinate-based data picking, the results of the present study got compared with both those of G93 and the T-SHM project regarding ten earthquake-prone cities surveyed. The data and materials used in this research are available from the corresponding author upon reasonable request.

4 Method and limitations

In this part of the paper, for the sake of brevity, the full details of the Bayesian procedure used in this study are not fully reported. Instead, only the basics of the theory and its pertinent formulations are solely given to illustrate what the methodology aims to represent. For an in-depth description of the theory, the following papers that refer to the original sources are strongly recommended to readers. Besides, to the best of our knowledge, only two examples (Lyubushin and Parvez 2010; Salahshoor et al. 2018) used the way of Bayesian estimation philosophy implemented here exist in the literature, and it is worth noting that these early examples will benefit the reader as well. With this in mind, the summary of the Bayesian theory is given hereunder.

We call "R" as an acronym that denotes a value referring to either estimated or measured quantity observed in an apparent sequence happened in a particular period commonly named as the past time interval ($-\tau$, 0):

$$\overrightarrow{R}^{(n)} = (R_1, \ldots, R_n), R_i \geq R_0, R_\tau, R_\tau$$
$$= \frac{\max}{1 \leq i \leq n} (R_1, \ldots, R_n) \tag{1}$$

This sequence (1) is nothing but a time series and each member of which could hypothetically be found in a random space posed by a kind of coincidence-based physical nature. In other words, no discretionary event is thusly considered.

The sequence of $\overrightarrow{R}^{(n)}$ is considered to be either a bin of the magnitudes of seismic events that occurred in an enclosed region or the logarithm (to the base 10) of the peak ground accelerations ($A_{\max}$ or hereafter referred to as PGA) of those seismic events measured within the scope of the specified area.

R_0 is a specific quantity called minimal cutoff value, which is either determined by physical possibilities of strong ground-motion recording network or else it is picked out as an ordinary but statistically representative value from those events of the sequence (1). As a fundamental and constructive assumption for the whole theory, the sequential values of (1) follow the Gutenberg–Richter (G-R) power law for magnitude-recurrence (Gutenberg and Richter 1944). Now then, we can write the parametric equality below.

$$\Pr\{R < x\} = F(x|R_0, \rho, \beta)$$
$$= \frac{e^{-\beta.R_0} - e^{-\beta.x}}{e^{-\beta.R_0} - e^{-\beta.\rho}}, R_0 \leq x \leq \rho \tag{2}$$

The upper limit of (2), ρ, denotes the maximal possible value of R that has an unknown parametric quantity. In similar ways, another parameter is β, which denotes the slope of the G-R law computed from a doubly logarithmic plot.

The second assumption of the theory, which is a rather requisite thought in explaining the sequence of the earthquake occurrence both in time and space, is about the sequence (1) that it expresses a Poissonian statistical process driven by λ. In the meanwhile, λ is a distribution-oriented well-known intensity parameter and then it comes out as another unknown parameter to the theory.

If we gather the unknown parameters up here, the full vector of the unknown parameters can be written as follows:

$$\theta = (\rho, \beta, \lambda) \tag{3}$$

For brevity, all explanatory expressions can be summed up regarding the given sequence (1), and then the argument R_0 is omitted and we can express them in nature of $\cdot(\cdot \mid \theta)$, namely, for (2), the expression turns to $F(x| \theta)$. Considering the law (2), the probabilistic density function of the distribution can then be written as

$$f(x|\theta) = F'(x|\theta) = \frac{\beta.e^{-\beta.x}}{e^{-\beta.R_0} - e^{-\beta.\rho}} \tag{4}$$

Let ε be an error term for the known values of sequence (1). That is to say, the magnitudes of the earthquakes in the sequence (1) do not include the *true* values; in fact, they are nothing but the *apparent* values of R. Hence, they, apparent values, can be represented as follows:

$$\widetilde{R} = R + \varepsilon \tag{5}$$

Now, then, we can introduce the $n(x| \delta)$ explaining the error's (ε) probabilistic distribution density and δ is a set scale parameter regarding the density. At this juncture, we can thence start using the below distribution density in a uniform nature,

$$n(x|\delta) = \begin{cases} 1/2\delta, & |x| \leq \delta \\ 0, & |x| > \delta \end{cases} \quad (6)$$

We can also assign $\prod$ as a priori uncertainty to each parameter of θ, considering that a priori density of θ is of uniform nature:

$$\prod = \left\{ \lambda_{\min} \leq \lambda \leq \lambda_{\max}, \beta_{\min} \leq \beta \leq \beta_{\max}, \rho_{\min} \leq \rho \leq \rho_{\max} \right. \quad (7)$$

The future time interval $[0, T]$ is a temporal array that becomes our working space to be used to delineate ρ and its quantiles.

To the definition of conditional probability, a posterior density of distribution of θ can be represented below by the Bayes formula (Rao 1965);

$$f\left(\theta | \overrightarrow{R}^{(n)}, \delta\right) = \frac{f\left(\theta, \overrightarrow{R}^{(n)} | \delta\right)}{f\left(\overrightarrow{R}^{(n)} | \delta\right)} \quad (8)$$

Formula (8) is the principal estimation tool for a posterior parametric density of θ.

The Bayesian estimate of vector θ is then given below:

$$\widehat{\theta}\left(\overrightarrow{R}^{(n)} | \delta\right) = \int_{\Pi} \vartheta \cdot f\left(\vartheta | \overrightarrow{R}^{(n)}, \delta\right) d\vartheta. \quad (9)$$

In this implementation of the theory, $\rho_{\min} = R_\tau - \delta$. $\rho_{\max}$ is set up by the user subjecting to the nature of the series (1). Maximal and minimal boundary values can be expressed in below forms:

$$\beta_{\min} = \beta_0 \cdot (1 - \gamma), \beta_{\max} = \beta_0 \cdot (1 + \gamma), 0 < \gamma \leq 1 \quad (10)$$

In formula (10), β_0 is the median value computed from the G-R law through the maximum likelihood estimation technique:

$$\sum_{i=1}^{n} \ln \left\{ \frac{\beta \cdot e^{-\beta \cdot R_\tau}}{e^{-\beta \cdot R_0} - e^{-\beta \cdot R_\tau}} \right\} \rightarrow \max_{\beta, \beta \in (0, \beta_\delta)} \quad (11)$$

β_s is a fairly large value, e.g., 10, γ is a parameter of the method taken to be 0.5.

As with the Poissonian process particularly for significantly large n (Cox and Lewis 1966), the variance of λ_τ tends to have approximate value; $\sqrt{n} \approx \sqrt{\lambda \tau}$.

If we draw the boundaries for our estimations (upon $\pm 3\sigma$), we can procure the below expression for the intensities denoted in (15):

$$\lambda_{\min} = \lambda_0 \cdot \left(1 - \frac{3}{\sqrt{\lambda_0 \tau}}\right), \lambda_{\max} = \lambda_0 \cdot \left(1 + \frac{3}{\sqrt{\lambda_0 \tau}}\right) \quad (12)$$

where $\lambda_0 = \frac{\overline{\lambda}_0}{c_f(\beta_0, \delta)}, \overline{\lambda}_0 = \frac{n}{\tau}$.

It is particularly presented to the reader's attention that the fundamental philosophy of Pisarenko et al. (1996) conceptually uses a commonly known fundamental approach postulated by Cornell (1968) and McGuire (2004) to seismic hazard analysis. The significant difference between the Bayesian theory used in the current study and the Cornell–McGuire version is attributed to both the arrangement of earthquake sources and the computation of the source parameters. Namely, in the Bayesian approach of Pisarenko et al. (1996), the corresponding parameters to the theory (ρ, β, λ) are thought to have a succession denoting logarithm of acceleration values from adjoining events.

Using the GMPEs, β and λ values, which are of similar nature with the other seismicity parameters to the theory, are calculated through the acceleration values. More precisely, magnitude values are replaced with the peak ground acceleration (to the logarithm scale) values calculated by replacing the magnitude and distance in GMPEs. Thus, this method indeed offers a significant convenience to the frequently rising question of whether or not the seismogenic zonation, in other words, any zone-dependent assumption is needed. That is to say, neither local nor regional seismic sources are used to obtain PGA estimates.

Right then, according to the Bayesian methodology briefly outlined above, we estimated the parameter "ρ" that epitomizes the maximal anticipated value of PGA upon a probability ($\alpha = 0.90$) for a predefined future time interval ($T = 475$ years) in a spatial area covering both Turkey and its proximity gridded into 200×200 nodes. The corner limits of the spatial boundaries of the catalog are $32° \leq \text{Lat} \leq 45°$; $23° \leq \text{Lon} \leq 48°$. However, the boundaries of the study area covering mainland Turkey are $35.81° \leq \text{Lat} \leq 42.10°$; $25.67° \leq \text{Lon} \leq 44.82°$. In that sense, the spatial boundaries of the Turkish hazard map are considered to be of a clipped version of the outer limits of the catalog. As is inferred from the limits above, the spatial coverage of the catalog, which particularly elongates to the off places from the boundaries of Turkey, gives us a useful advantage over the particular use of in-field data only for Turkey. Seeing that possible sharp interruption of the spatial and temporal data in the proximity of any study area possibly

causes significant errors in geostatistical correlations and, in the strict sense, it could yield erroneous numerical extrapolations. As for computation practices, the path that we followed for the estimations can be summarized as follows. For each grid, the PGA sequence was computed through the catalog of earthquakes and specified GMPEs (AC10, AK14, and CY08 with weights of 1/3). As is aforementioned, these relationships and weights are the same as those used by the T-SHM project.

For making the Bayesian estimates of PGA possible for a given future time interval according to Lyubushin et al. (2002), the solely major independent events of each node are needed to get included to the Bayesian framework, which is crucial for satisfying the characteristic Poissonian behavior assumption of the sequence. In this vein, the dependent events are needed to be first identified and then removed from the catalog to achieve the fortuitous sequential characteristics of time moments. Surprisingly, very little work has as yet been done on the issue of which declustered method is the most applicable one and rather is of better result-giving performance regarding the seismicity of Turkey, albeit the number of studies is in the ascendant. To the best of our knowledge, in this regard, two studies are now only available in the literature. On the one hand, in a sensitivity-based study, Eroglu Azak et al. (2018) investigated the effects of different mainshock catalogs derived from several seismic declustering methods. On the other hand, through the agency of simulation envelopes and Monte Carlo tests particularly to keep track of the variations in the temporal and spatial point patterns, Nas et al. (2019) made a spatiotemporal comparison of different mainshock catalogs derived from several declustered methods. Apart from many other findings, the results of each study revealed that the Gardner and Knopoff (1974) method was found to be fairly effective in giving a better-refined catalog. In this respect, the full earthquake catalog used in this study got then declustered by the Gardner and Knopoff (1974) method with a purpose-oriented modification to a slight extent. Gardner and Knopoff (1974) put forward to a kind of windowing method that mainly classifies earthquakes according to their spatial and temporal characteristics. Each window, either spatial or temporal, is based on magnitude. Namely, the method progresses based on magnitudes and presents magnitude data. The modification is nothing but an extra query on deciding by which event should be adopted as a mainshock only to be used

in the computations of PGA values. More precisely, being the first step of declustering, all of the events were divided into two distinct classes—mainshocks and their fore- or aftershocks—with the help of the Gardner and Knopoff (1974) method. Now that the aim of the modification is first to find and then leave one event only in a reciprocal earthquake sequence, the magnitude of this single event must have characteristics to deliver the highest acceleration values depending on the GMPE used. Hence, only one event was left from each mainshock and aftershock sequence that generates the largest PGA. Thanks to this application, the possibility of auto-eliminating a large aftershock that could produce larger PGA values than its hypothetical mainshock got eliminated. Early examples of this implementation are available in Lyubushin et al. (2002) and Lyubushin and Parvez (2010). On the upshot, the resultant catalog of independent events consisted of 7275 earthquakes. For each node of the grid, only 30 events of "mainshocks" with maximum PGA values were specified for the subsequent analyses. The choice of 30 events has so far been checked a lot of times and to have been judged as quite sufficient enough numbers for estimating statistics of maximum events (Bayrak and Türker 2016; Bayrak and Türker 2017; Mohammadi et al. 2016; Pisarenko and Lyubushin 1997; Pisarenko et al. 1996; Salahshoor et al. 2018; Tsapanos et al. 2001; Yadav et al. 2013b). The method that we used here is principally intended for estimating maximum events, all other events (not maximum) are necessary only for estimating the b value. The convergence of the Bayesian method is presented in the prominent book of Rao (1965). In our example, the volume of the priory domain was even too much and according to the theorem of convergence of the Bayesian method, the influence of a priory method is tending to zero with the increasing number of observations for which case of $N = 30$ is quite enough. All things considered, we ultimately achieved the quadrat value ($n = 30$) in relation (1), albeit with different values of R_0 and $R_\tau = \overset{\max}{} 1 \leq i \leq n R_i$, namely the a priori threshold value for ρ was adopted as $\rho_{\max} = R_\tau + 0.5$. Furthermore, in this methodology, if there are no 30 events that produce the peak ground acceleration in the grid point that exceeds a given threshold, then this grid point, which scilicet epitomizes a sparse seismicity characteristic, is first omitted from the analysis. But, be that as it may, the value of PGA statistics nevertheless is estimated in this grid point by extrapolating from nearest

other grid points using a smoothing method called Gaussian kernel function with radius 1° using 100 nearest neighbors' values. In a more succinct sense, on the basis thereof, by dividing all study area into 200 × 200 orthogonal regular grids, it is possible to make a map that depends upon stationary quadrat counts as specified and explained above. Upon these node-based calculations, the grid values got converted to the maps with the help of a non-parametric smoothing process depending on the Gaussian kernel functions (Härdle 1990). The World Geodetic System (WGS84) was used as a reference coordinates system for all coordinate-based products produced in the context of the present study.

5 Results and discussion

Using the GMPEs mentioned above weighted equally with the ratio of 1/3, Fig. 3 shows the seismic hazard map of 90% quantile of the distribution of PGA values (in g) for the 475-year return period, which is another expression of 10% probability of exceedance in 50 years according to Poisson distribution. Figure 3 is an unclipped but processed map and it covers both the inland and seas encompassing Turkey, which constitutes the full orthogonal space of the research area. After having clipped the inland of Turkey from the total map of hazard, we created the bare PGA hazard map of the inland of Turkey (Fig. 4) through the methodology of which is the same with that of T-SHM project. On the one hand, the map depicted in Fig. 4a is a smoothed contour map, and it was identically made through the same philosophy that the T-SHM project used regarding the mapping concept. On the other hand, Fig. 4b shows the same hazard map, namely that was created with the same data of Fig. 4a, albeit using a zonation methodology in line with a technique that the 1° radius used. The active fault map of Turkey depicted as a layer in the pertinent hazard maps below was taken from Emre et al. (2013).

In examining Fig. 4, regarding the full extent of Turkey, the maximum PGA values were observed in some specific cities (Erzincan, Düzce, Sakarya, and Kocaeli), all of which are located in the NAFZ. The PGA values estimated for throughout NAFZ were observed greater than 0.2g overall. It is worth noting that the locations for which high PGA values estimated are those places where the most destructive earthquakes occurred in Turkey to date, for instance, 27 December

1939 Great Erzincan Earthquake (M7.6, Ms7.9), 17 August 1999 Kocaeli (M7.6), and 12 November 1999 Düzce (M7.1) earthquakes. The estimated PGA values for the eastern Anatolia zone varied from 0.1 to 0.2g. In particular, the estimated PGA values along with the EAFZ were found to generally be less than 0.4g and the largest values in this region were observed in and around the Karliova region that comprises a non-subductable intercontinental junction commonly called "Karliova triple junction." More so, it is a spectacularly engrossing geologic formation, which gets the Anatolian, the Eurasian, and the Arabian plates to come together (Aktug et al. 2013; Barka 1992; Şengör 2014). In addition, a significant hot spot was observed on the east coast of Lake Van where is of a recently delineated rupture process (Altiner et al. 2013; Elliott et al. 2013; Konca 2015; Utkucu 2013) due to the 23 October 2011 Van earthquake (M7.1). The PGA values calculated for the western Anatolia region generally were found to be between 0.3 and 0.4g. Moreover, the values in the border region among the cities of Burdur, Isparta, and Denizli were apparently observed to be larger than 0.4g. This hot spot location was found to be consistent with the particular location where the 03 October 1914 Burdur earthquake (M6.9) happened. The seismic hazard potential of the Central Anatolia region was observed indeed low ($< 0.2g$). Also, when moving away from the middle of the Central Anatolia ($< 0.1g$) to the places having significantly active seismic zones, which encompass thereto, estimated PGA values increased and finally reached to the largest value (0.586g) to the scale. Of the cities located in the central part of Turkey, in the western tip of the Kirsehir and the southern tip of the Osmaniye, the sharp PGA increase was observed. These locations were found to be consistent with those of the 19 April 1938 Kirsehir earthquake (M6.5) and several other moderate earthquakes happened on the southern tip of the EAFZ. Southernmost border cities of Turkey were found to be the lowest seismic hazard zones, which are similar to those cities most of which are located in the northern cities of Turkey. To the best of our knowledge, the main reason for these low PGA values, as is seen in Fig. 4, is thought to be not only ascribed to the relative tectonic activity of particular geological structures but also the fact that these structures have long been undergoing creep-driven movements. Furthermore, it is worth noting that both the locations and the number of active recording stations belonging to the seismograph networks of Turkey are crucial elements
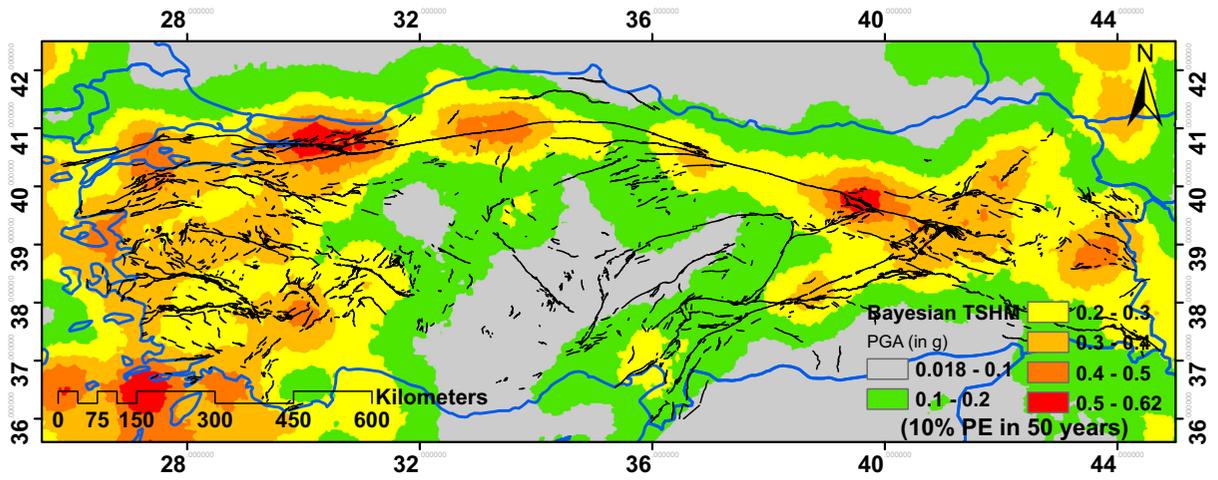
Fig. 3 Unclipped version of Bayesian Turkish seismic hazard map (B-TSHM) with spatial zonation (upon 90% quantile, $V_{S30} = 760$ m/s, 475-year return period, in *g*) covering both seas and lands
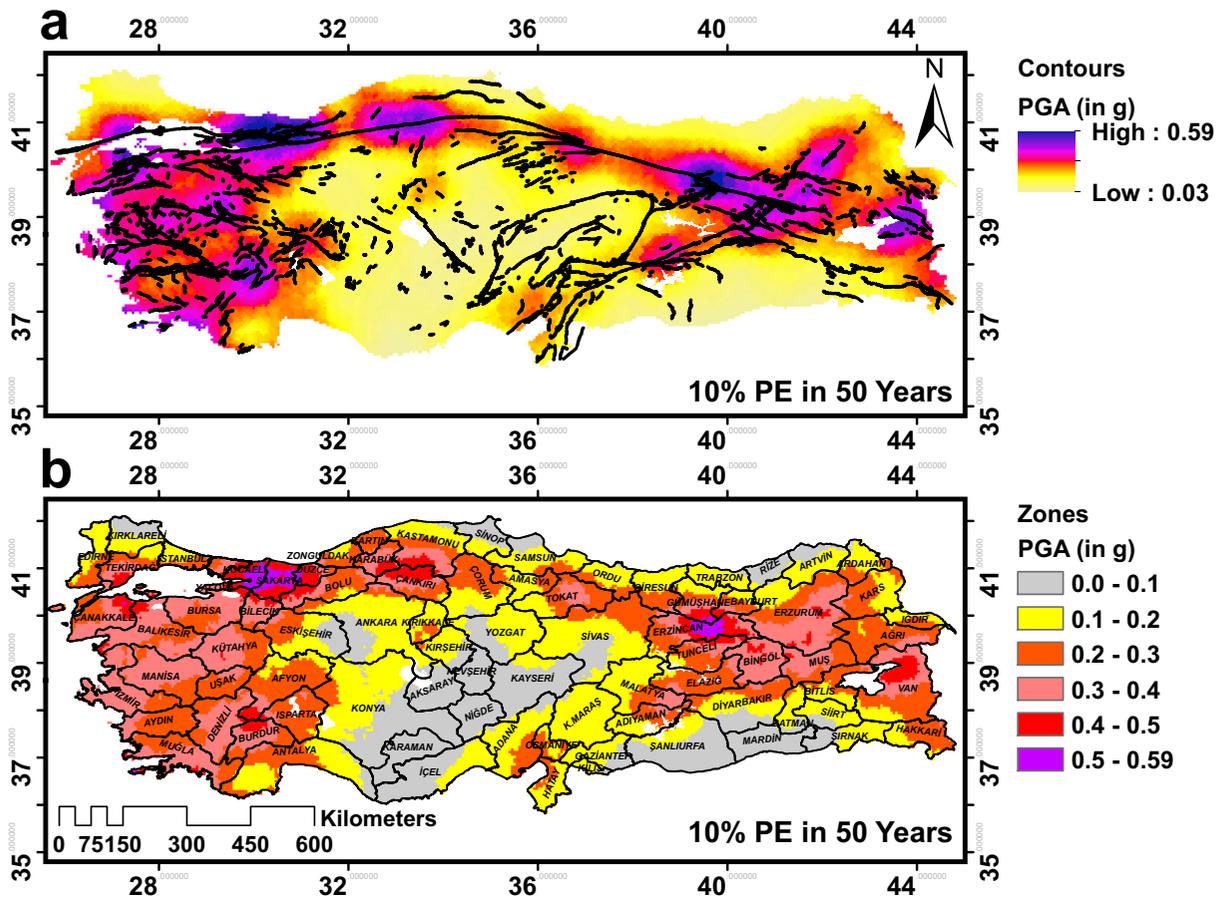
Fig. 4 Bayesian Turkish seismic hazard map (B-TSHM) covering the inland areas only (upon 90% quantile, in *g*). **a** The map of smoothed contours. **b** The map of spatial zonation. The estimations are subject to reference-rock site assumption ($V_{S30} = 760$ m/s) and are made through a three-pronged logic tree, which comprises AK14, AC10, and CY08, depending on the 475-year return period

in the sound analysis of strong ground-motion parameters of each earthquake. Upon the increases in these instruments, the sensitivity of the observations and straightforwardness of calculations increase as well. Therefore, the uncertainty created by the increased sensitivity over time affects this kind of seismic hazard studies one way or another. That is to say, this effect will inevitably be observed in future studies. At exactly this point, the issue of why we did not use historical earthquakes (prior to 1900) can clearly be explained. First of all, as is explained above, Salahshoor et al. (2018) signified that the Bayesian method of Pisarenko et al. (1996) gives more healthy and straightforward outputs if the earthquake catalog to be used as a main input to the method is spatially and temporally complete. Instrumental catalogs are of an apparent spatial and temporal continuity, although there are some data-related problems in itself, for instance, the sensitivity of magnitude precision and lack of the number of measurements. However, combining historical earthquake catalogs with instrumental catalogs in order to use in hazard estimates is a rather problematic issue nevertheless, because the magnitudes of these historical earthquakes were totally anticipated through several non-objective historical records and few if any geologic data. It is a well-known fact that a consistent and unbiased earthquake catalog is a must-have factor for the success of the hazard estimates. Namely, due to indispensable conversions of the macroseismic intensities to a kind of instrumental magnitudes, they obviously increase the rate of the uncertainty of the instrumental catalog to be used in hazard estimates (Rong et al. 2011).

In fact, all of the estimated PGA values and hazard maps were made taking into account the reference-rock site condition characteristics, which made our results comparable to the predecessor and successor hazard maps of Turkey. Namely, Akkar et al. (2018a) stated that the PGA hazard maps of the T-SHM project were created in view of the reference-rock site conditions. Also, they expound with the justification that because the G93 solely used the GMPE of Joyner and Boore (1981), which does not include the site-specific term, G93 compulsorily disregarded site effect in the calculations. However, Akkar et al. (2018a) also stated that the result of G93 should be ascribed to the statement of G93 that denotes the use of apparent stiff soil characteristics in computations. Consequently, they signify that the maps generated by G93 should be interpreted to have

been prepared with respect to the boundary of stiff soil and rock site condition. This way of thinking is attributed to the B/C boundary of NEHRP (BSSC 2001) classification of soil sites, which is consistent with the adoption of reference rock site condition both in the present study and in the T-SHM project. In a nutshell, this joint feature helps us compare them with each other.

The contour map of PGA ratios [PGA(this study)$_{Long, Lat}$/PGA(G93 and T-SHM)$_{Long, Lat}$] shown in Fig. 5 denotes that the Bayesian seismic hazard map of the present study makes larger PGA estimates, which have been up to 20–45% with regard to G93, in several particular places (Erzincan, Kocaeli, Sakarya) where the major earthquakes of Turkey occurred to date and further where the main active faults are abundant. Besides, these locations represent the highest acceleration values of the B-TSHM (see Figs. 3 and 4b). As moving away from these hot spots, the calculated PGA ratios decreased following the significant contours, which are available at the approximately same distance to these points that epitomize the explicit attenuation. Of the PGA ratios expressed in Fig. 5, in several places, such as Erzurum, Erzincan, Yozgat–Sivas border, Tekirdag, the northern tip of Edirne, and in a spatial band of the Asian side of Istanbul city to Duzce, the computed ratios were found to be 20% larger than those of G93 and they mostly observed in the proximity of the hot spot places aforementioned. Besides, in the Kocaeli–Sakarya band, and in the cities of Bilecik, Gumushane, and Van, B-TSHM gave much higher acceleration values than those of T-SHM. As moving away from the center of Kocaeli–Bilecik cities, in the middle of the triangle formed by Karabuk, Kastamonu, and Bartin cities in parallel to the NAF, in the city center of Kirsehir and Erzincan, on the axis of Gumushane–Bayburt, between eastern Erzurum and western Kars, between Van and Agri city center, B-TSHM gave higher acceleration values than those of T-SHM. When moving away from these areas, a certain attenuation pattern appeared and the PGA values of B-TSHM gradually fell below the values of T-SHM. Meanwhile, an interesting finding is that the PGA values of B-TSHM were rather in line with the acceleration values given by T-SHM and those of G93 too. In Fig. 5, according to both maps, it is observed that the results of this study are compatible in the ± 20% band in the cities of Tekirdag–Canakkale, Kutahya, Burdur, Kastamonu, Tokat, Yozgat, Gumushane, and Erzurum. Right after the pertinent PGA ratios observed in these regions, the ratios decreased by up to 20%. This
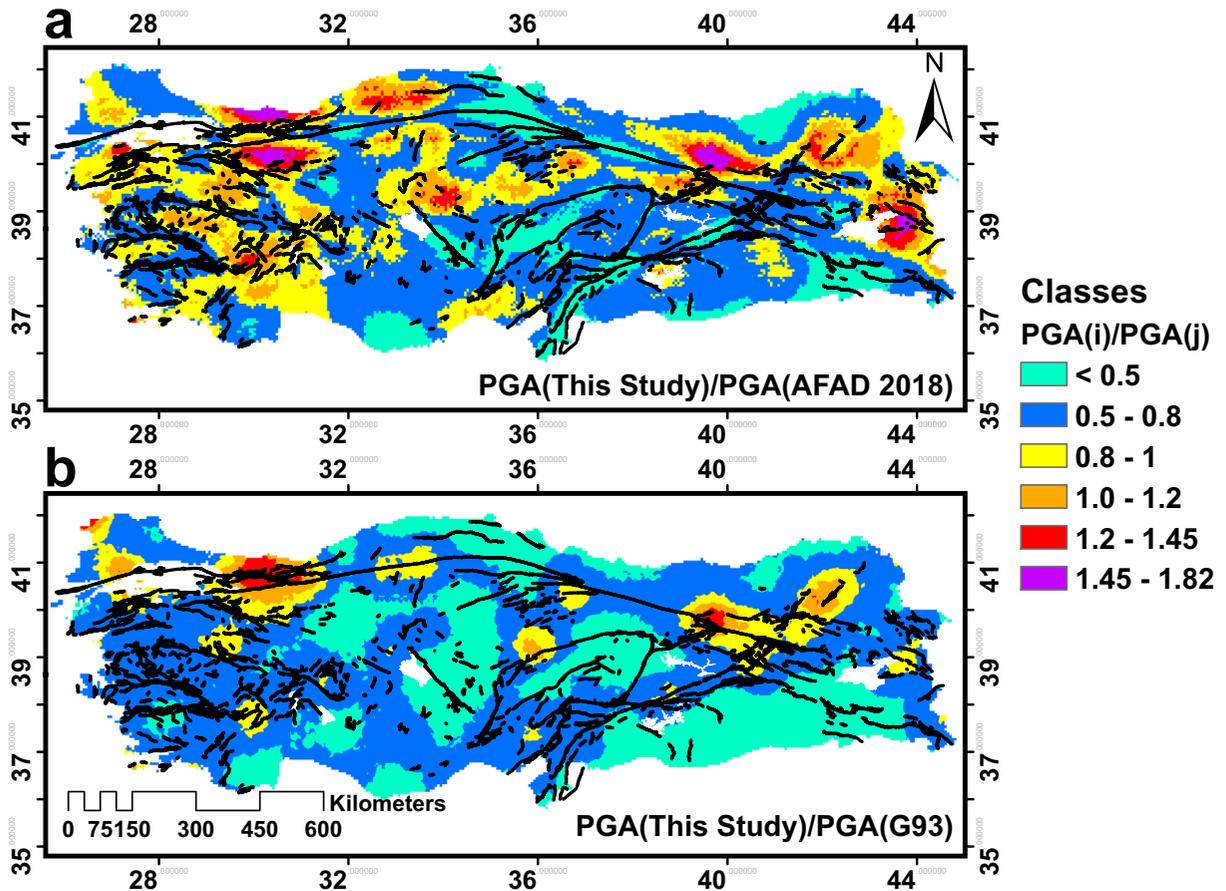
Fig. 5 Smoothed contour maps of the normalization ratios **a** for AFAD (2018) and **b** for G93 (each map evaluated in this plot is based on the 475-year return period and comprises the reference rock ($V_{S30} = 760$ m/s) site-oriented PGA estimates)

is a strong indication of the fact that the estimates of the B-TSHM reasonably corresponded to the expected attenuation characteristics of the peak ground acceleration against increasing JB distance. Furthermore, almost a large part of the Aegean region, some part of Eastern Anatolia, particularly in the East Anatolian Fault Zone, the PGA ratios decreased by 50–80% relative to G93. When it comes to T-SHM, B-TSHM gave much closer results to it in these regions, especially in active seismic zones with a large number of fault bundles. In the rest of the country, most of which cover the cities located in the northern and southern border of Turkey and Central Anatolia, where the large earthquakes either not realized or rarely happened to date, the PGA ratios of B-TSHM decreased by 50% or less than that of G93. To put it in another way, these areas might specifically have corresponded to the regions that have not so far produced any large earthquake due to either veiled fault creep or the very sparingly placed or even the absence of

recording stations, as in Northeast Turkey (Softa et al. 2019). As can be seen above, the interpretations were mostly made by taking into consideration the places where the significant and densely flocculated earthquakes happened. The main reason for this is that the method used in this study is not based on any kind seismogenic fault; that is, in point of fact, it is rather based on the use of earthquakes themselves. In the strictest sense, because the T-SHM project was conducted using several kinds of areal sources for crustal events and active faults (Akkar et al. 2018a), it is reasonably expected that the certain ratios are thence observed in or around the specified fault areas. However, in the present study, as is ideally and distinctively expected, the self-similar ratios are observed and found to have intensified at the specific locations where the earthquakes occurred with similar PGA values. Succinctly, the reasons for low PGA values expressed in B-TSHM can somewhat be attributed to several factors reviewed in above

paragraphs such as the lacking seismometer, aseismic creep, inherited geological structures, and/or multifarious combinations of these factors. In addition, the main reason for the moderate to much higher values of B-TSHM cannot be attributed to a single factor; howbeit, it could be related not only to explicit instrumental seismicity hereby covered but also whether the historical seismicity got evaluated or not. An individual sensitivity study might also be required to illuminate this, which could also be considered as a pioneering example for all other future studies.

The query on whether or not the similarity of the empirical tail probability function of the estimated PGA values to the G-R recurrence law exists is one other collateral objective of this paper. From this standpoint, Fig. 6 shows the individual empirical tail functions of distribution of calculated PGA values (in the form of Log(g)) according to three GMPEs of AK14, AC10, and CY08 considering city center coordinates of ten earthquake-prone cities of Turkey. Regarding the city center–based computations, these coordinates were taken as geographical coordinates of the locations where the governor's office is located. As can be seen in Fig. 6, while GMPEs of AK14 and CY08 have a very similar and mostly overlapped increment pattern, the AC10 generally proceeds with some less but approximately the same slope.

In the context of this paper, it is, of course, not possible to provide all the maps that could be created depending on several different return periods using hereby adopted Bayesian technique regarding both for the purpose of the study and the brevity of thereto. But, be that as it may, Fig. 7 denotes a panel plot of the individual quantiles of expected PGA values (in g) created for 43, 72, 140, and 475 years of return period for surveyed ten cities of Turkey respectively. In some regions with very high seismicity (e.g., Bingol, Erzincan, Izmit, Tokat), the trends of estimated PGA values were distinctive to the eyes that the PGA values increased rapidly with the increasing return period. Besides, some cities (Izmir, Istanbul, Agri) followed a slight PGA increment against the increased return period. Having said that, the estimated PGA values for the 475-year return period were very close to those values estimated for the rather extended return periods. This pattern can also be attributed to the decreased possibility of making a straightforward projection with the catalog when the PGA estimations are particularly made taking into account a very long return period. Now that the

catalog, which was used in the T-SHM project and used in this study with a somewhat improvement, covers the earthquakes that happened in slightly more than a century (1900–2018), this problem has distinctly been available in both studies.

Figure 8 shows the maximum expected PGA values (in g, upon 90% quantile) determined in this study for selected ten cities by taking into account the 475-year return period comparing with the values picked from the maps of G93 and T-SHM project regarding the same spatial coordinates. From this point on, the PGA values estimated for Istanbul City by each study were found to be very close to each other. In general, it can, therefore, be said that the T-SHM project overall tends to make higher estimates against those estimated by G93 and this study. Furthermore, for some cities, the results of the present study exceeded the PGA values suggested by the G93, while, on the other hand, for some cities, it was the opposite. Therefore, it is evident that even if the expected values contain somewhat differences, similar estimates got observed in the same region, excluding the city of Izmit.

6 Conclusions

With causalities and loss of property in the headlines almost every year, the issue of the intrinsically ever-changing seismic hazard potential of countries is taking on increasing importance, especially for the survival of the future of nations. Of several different methodologies developed and implemented to date, the present study is the first example of the Bayesian method of Pisarenko et al. (1996), which directly uses the PGA values to estimate the seismic hazard, for Turkey. In that sense, we aimed at determining PGA values with the context of different return periods and then comparing them with the results of the antecedent and current national seismic hazard projects of Turkey. In essence, comparing with the T-SHM project, which is a large-scale study ever conducted for this purpose in Turkey, the scope and the details of the current study remain relatively limited though. Besides, this study fundamentally tests whether the Bayesian method of Pisarenko et al. (1996) is suitable for Turkish seismicity and what the differences and similarities between the outcomes of the present study and those of early ones are. However, if we pay attention to the spatial distribution characteristics of PGA values over the maps compared here, the
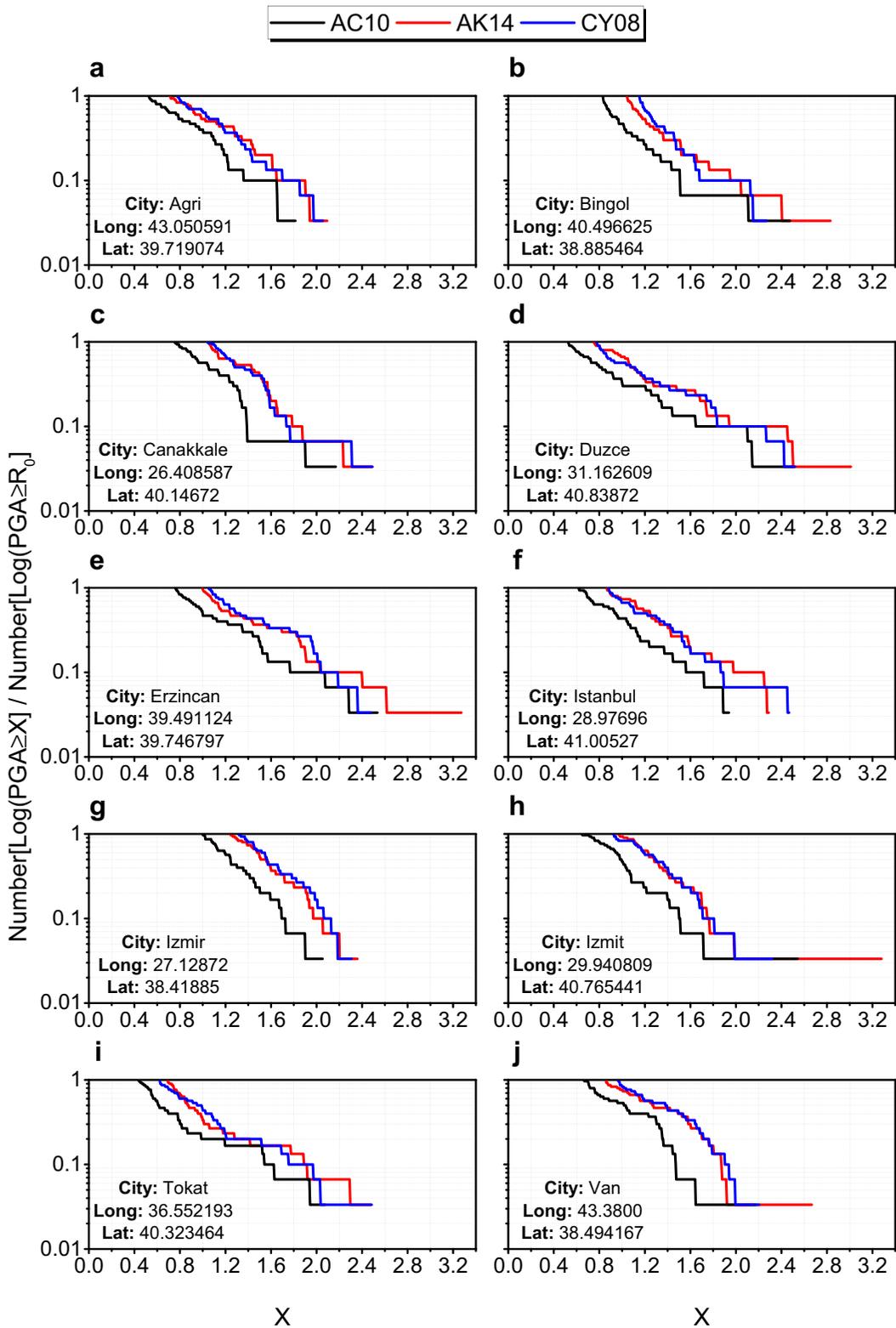
Fig. 6 **a**–**j** Empirical tail probability functions of PGA distributions (for 475-year RP and $V_{S30} = 760$ m/s, in *g*) for ten earthquake-prone city centers concerning AK14, AC10, and CY08 respectively
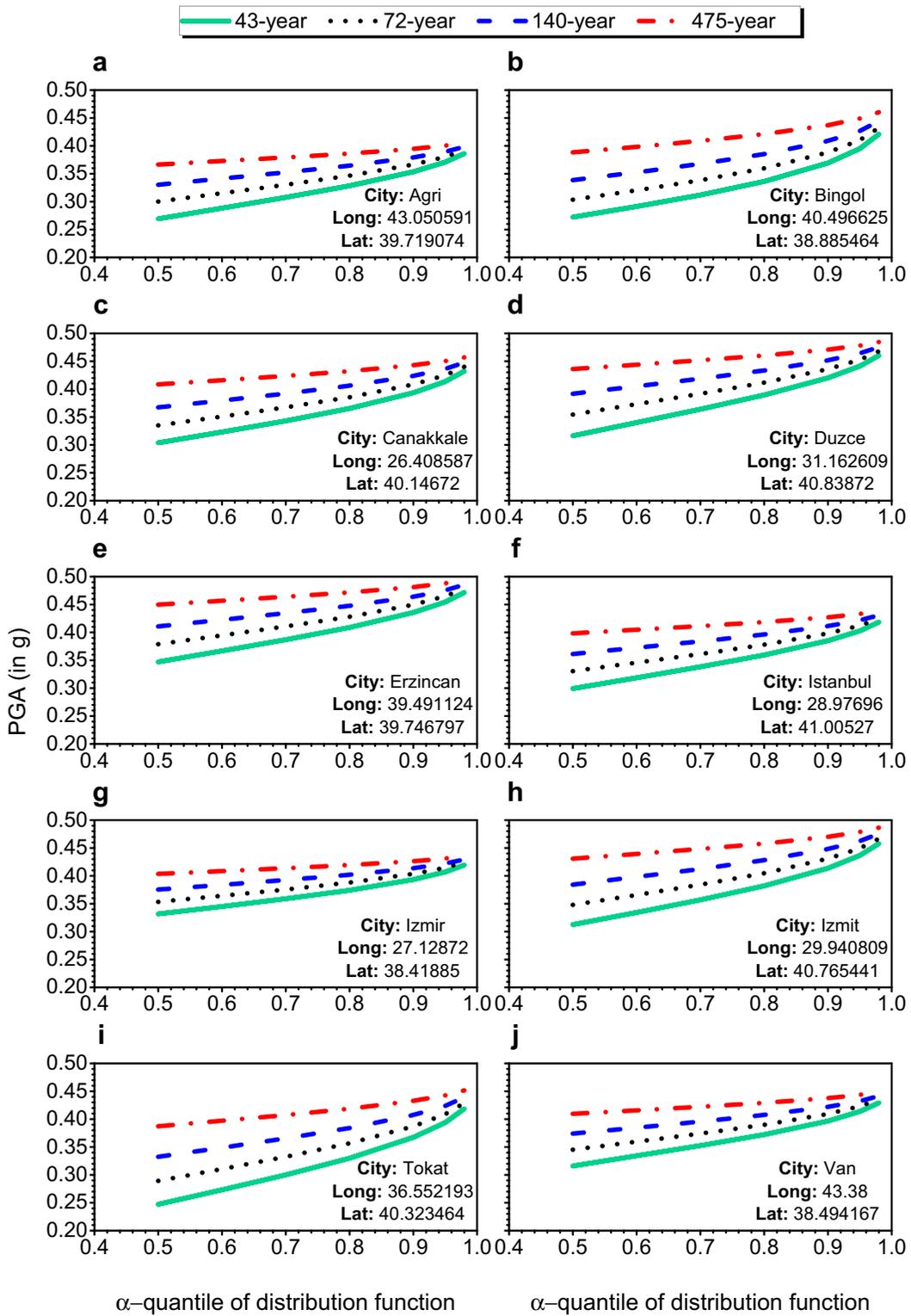
Fig. 7 a–j The quantiles of the distribution function of estimated PGA values (in *g*, upon 90% quantile) for ten earthquake-prone cities of Turkey (the curves represent the expected PGA values depending on 43, 72, 140, and 475 years of return period and $V_{S30} = 760$ m/s)
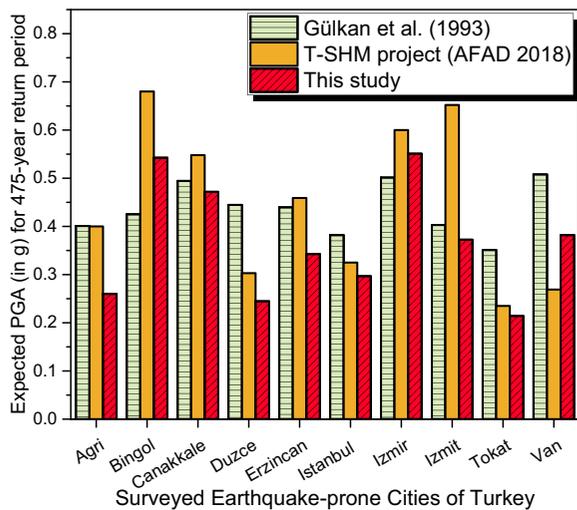
Fig. 8 Comparison of the maximum expected PGA (upon 90% quantile, in *g*) for ten earthquake-prone cities of Turkey (all of the PGA values are calculated by taking into account the reference-rock site condition ($V_{S30} = 760$ m/s) and a return period of 475 years)

boundaries of the spatial distribution of PGA values determined in the present study are found to be quite close to those of G93 and T-SHM project. It is not possible for a certain amount of difference or departure between any different studies not to occur. This fact is clearly seen when the maps of the G93 and the T-SHM get compared.

Another conclusion that can be drawn from the present paper is that the Bayesian method of Pisarenko et al. (1996) is thereby referred to as an alternative and straightforward tool for further seismic hazard analyses for Turkey. One of the several pros of this method is that the Bayesian method does not require the use of areal or line faults. As is known, unavoidable uncertainty in defining the space and time of an earthquake is likely. Therefore, the use of a distribution function is a genuine convenience of the method in the estimation of ground-motion amplitudes. One of the few if any cons of this method is that the method of Pisarenko et al. (1996) requires seismic catalog and GMPEs only. Considering that the method is not zone-dependent but catalog-driven, it is possible to specify in conclusion that the earthquakes themselves are a reasonably sufficient and versatile tool to elucidate the potential seismic hazard peculiar to a given region. Thus, much more precise detection of earthquake locations, magnitudes, and other related parameters can ultimately help us to make a less biased and more accurate evaluation of potential seismic

hazard for the zones where significant and intensified seismicity is available. To provide reliable data for all kinds of seismic hazard studies, it is highly recommended that such studies should be supported and their findings should particularly be compared with those of paleoseismology studies to the utmost extent possible. In this sense, Paleoseismological and seismic studies should be carried out concurrently in terms of the quality and integrity of the information to be obtained, and thereby, total and inevitable bias on the hazard estimates can be reduced to the lowest possible levels.

It is evident and should particularly be emphasized here that the recent earthquake hazard map of Turkey (AFAD 2018), which is one of the most prominent figures of T-SHM project, will anywise not be superseded by the outputs of the present study, nor does our study have a motivation like this. However, the compendium of all the remarks of the current study clearly transpires that the method of Pisarenko et al. (1996) is genuinely applicable and feasible in estimating the potential seismic hazard of Turkey, while the number of the possible seismogenic zones is numerous, albeit self-amalgamated and contentious. With this study, it becomes clear that the holistic process of PSHA, which innately requires a long and tiresome effort, can instantaneously be performed against the changing of earthquake catalog over time and prompt evaluations can thus be made.

References

AFAD (2018) Earthquake hazard map of Turkey. The Disaster and Emergency Management Authority of Turkey

Akkar S et al (2018a) Evolution of seismic hazard maps in Turkey. Bull Earthq Eng 16:3197–3228. https://doi.org/10.1007/s10518-018-0349-1

Akkar S, Çağnan Z (2010) A local ground-motion predictive model for Turkey, and its comparison with other regional and global ground-motion models. Bull Seismol Soc Am 100:2978–2995. https://doi.org/10.1785/0120090367

Akkar S, Çağnan Z, Yenier E, Erdoğan Ö, Sandıkkaya MA, Gülkan P (2010) The recently compiled Turkish strong motion database: preliminary investigation for seismological parameters. J Seismol 14:457–479. https://doi.org/10.1007/s10950-009-9176-9

Akkar S, Kale Ö, Yakut A, Çeken U (2018b) Ground-motion characterization for the probabilistic seismic hazard assessment in Turkey. Bull Earthq Eng 16:3439–3463. https://doi.org/10.1007/s10518-017-0101-2

Akkar S, Sandıkkaya MA, Bommer JJ (2014) Empirical ground-motion models for point- and extended-source crustal earthquake scenarios in Europe and the Middle East. Bull Earthq Eng 12:359–387. https://doi.org/10.1007/s10518-013-9461-4

Aktug B, Dikmen U, Dogru A, Ozener H (2013) Seismicity and strain accumulation around Karliova triple junction (Turkey). J Geodyn 67:21–29. https://doi.org/10.1016/j.jog.2012.04.008

Allen CR (1982) Comparisons between the North Anatolian Fault of Turkey and the San Andreas Fault of California. In: Işikara AM, Vogel A (eds) Multidisciplinary approach to earthquake prediction: Proceedings of the International Symposium on Earthquake Prediction in the North Anatolian Fault Zone held in Istanbul, March 31–April 5, 1980. Vieweg+Teubner Verlag, Wiesbaden, pp 67–85. https://doi.org/10.1007/978-3-663-14015-3_5

Altiner Y, Söhne W, Güney C, Perlt J, Wang R, Muzli M (2013) A geodetic study of the 23 October 2011 Van, Turkey earthquake. Tectonophysics 588:118–134. https://doi.org/10.1016/j.tecto.2012.12.005

Ambraseys NN, Jackson JA (2000) Seismicity of the Sea of Marmara (Turkey) since 1500. Geophys J Int 141:F1–F6. https://doi.org/10.1046/j.1365-246x.2000.00137.x

Badgley PC (1965) Structural and tectonic principles Harper & Row, New York

Barka A (1992) The north Anatolian fault zone. In: Annales tectonicae, . vol Suppl. pp 164–195

Bayrak Y, Türker T (2016) The determination of earthquake hazard parameters deduced from bayesian approach for different seismic source regions of Western Anatolia. Pure Appl Geophys 173:205–220. https://doi.org/10.1007/s00024-015-1078-x

Bayrak Y, Türker T (2017) Evaluating of the earthquake hazard parameters with Bayesian method for the different seismic source regions of the North Anatolian Fault Zone. Nat Hazards 85:379–401. https://doi.org/10.1007/s11069-016-2569-5

Bommer JJ (2012) Challenges of building logic trees for probabilistic seismic hazard analysis. Earthquake Spectra 28:1723–1735. https://doi.org/10.1193/1.4000079

Bozkurt E (2001) Neotectonics of Turkey–a synthesis. Geodin Acta 14:3–30

BSSC (2001) NEHRP recommended provisions for seismic regulations for new buildings and other structures, FEMA-368, Part 1 (Provisions): developed for the Federal Emergency Management Agency. Building Seismic Safety Council, FEMA, Washington

Campbell KW (1982) Bayesian analysis of extreme earthquake occurrences. Part I. Probabilistic hazard model. Bull Seismol Soc Am 72:1689–1705

Campbell KW (1983) Bayesian analysis of extreme earthquake occurrences. Part II. Application to the San Jacinto fault zone of southern California. Bull Seismol Soc Am 73:1099–1115

Chiou B-J, Youngs RR (2008) An NGA model for the average horizontal component of peak ground motion and response spectra. Earthquake Spectra 24:173–215. https://doi.org/10.1193/1.2894832

Cornell CA (1968) Engineering seismic risk analysis. Bull Seismol Soc Am 58:1583–1606

Cox DR, Lewis PAW (1966) The statistical analysis of series of events. Methuen's monographs on applied probability and statistics. John Wiley, London

Delph JR, Biryol CB, Beck SL, Zandt G, Ward KM (2015) Shear wave velocity structure of the Anatolian plate: anomalously slow crust in southwestern Turkey. Geophys J Int 202:261–276. https://doi.org/10.1093/gji/ggv141

Demircioğlu MB, Şeşetyan K, Duman TY, Çan T, Tekin S, Ergintav S (2018) A probabilistic seismic hazard assessment for the Turkish territory: part II—fault source and background seismicity model. Bull Earthq Eng 16:3399–3438. https://doi.org/10.1007/s10518-017-0130-x

Dewey JF, Hempton MR, Kidd WSF, Saroglu F, Şengör AMC (1986) Shortening of continental lithosphere: the neotectonics of Eastern Anatolia — a young collision zone Geological Society, 19th edn. Special Publications, London, pp 1–36. https://doi.org/10.1144/gsl.sp.1986.019.01.01

Duman TY et al (2016) Seismotectonic database of Turkey. Bull Earthq Eng 16:3277–3316. 1-40. https://doi.org/10.1007/s10518-016-9965-9

Duman TY et al (2018) Seismotectonic database of Turkey. Bull Earthq Eng 16:3277–3316. https://doi.org/10.1007/s10518-016-9965-9

Duman TY, Emre O (2013) The East Anatolian Fault: geometry, segmentation and jog characteristics vol 372. doi:https://doi.org/10.1144/SP372.14

Elliott JR, Copley AC, Holley R, Scharer K, Parsons B (2013) The 2011 Mw 7.1 Van (Eastern Turkey) earthquake. J Geophys Res Solid Earth 118:1619–1637. https://doi.org/10.1002/jgrb.50117

Emre Ö, Duman TY, Özalp S, Elmacı H, Olgun Ş, Şaroğlu F (2013) Active fault map of Turkey with an explanatory text. General Directorate of Mineral Research and Exploration, Ankara-Turkey

Emre Ö, Duman TY, Özalp S, Şaroğlu F, Olgun Ş, Elmacı H, Çan T (2018) Active fault database of Turkey. Bull Earthq Eng 16:3229–3275. https://doi.org/10.1007/s10518-016-0041-2

EPRI (2004) CEUS ground motion project final report 1009684. Electric Power Research Institute, Palo Alto

Eroglu Azak T, Kalafat D, Şeşetyan K, Demircioğlu MB (2017) Effects of seismic declustering on seismic hazard assessment: a sensitivity study using the Turkish earthquake catalogue. Bull Earthq Eng. https://doi.org/10.1007/s10518-017-0174-y

Eroglu Azak T, Kalafat D, Şeşetyan K, Demircioğlu MB (2018) Effects of seismic declustering on seismic hazard assessment: a sensitivity study using the Turkish earthquake catalogue. Bull Earthq Eng 16:3339–3366. https://doi.org/10.1007/s10518-017-0174-y

Galanis OC, Tsapanos T, Papadopoulos G, Kiratzi A (2002) Bayesian extreme values distribution for seismicity parameters assessment in South America. J Balkan Geophys Soc 5: 77–86

García D, Singh SK, Herráiz M, Ordaz M, Pacheco JF (2005) Inslab earthquakes of central Mexico: peak ground-motion parameters and response spectra. Bull Seismol Soc Am 95: 2272–2282. https://doi.org/10.1785/0120050072

Gardner JK, Knopoff L (1974) Is the sequence of earthquakes in Southern California, with aftershocks removed, Poissonian? Bull Seismol Soc Am 64:1363–1367

Guidoboni E, Comastri A, Traina G, Geofisica RINd (1994) Catalogue of ancient earthquakes in the Mediterranean area up to the 10th century. Istituto nazionale di geofisica Rome,

Gutenberg B, Richter CF (1944) Frequency of earthquakes in California. Bull Seismol Soc Am 34:185–188

Gülkan P, Koçyiğit A, Yücemen MS, Doyuran V, Başöz N (1993) A seismic zones map of Turkey derived from recent data. METU Civil Engineering Dept. Earthquake Engineering Research Center,

Härdle W (1990) Applied nonparametric regression. vol 19. Cambridge university press,

Harrison RW A (2008) model for the plate tectonic evolution of the eastern Mediterranean region that emphasizes the role of transform (strike-slip) structures. In: 1st WSEAS International Conference on Environmental and Geological Science and Engineering (EG'08) Malta

Hässig M, Duretz T, Rolland Y, Sosson M (2016) Obduction of old oceanic lithosphere due to reheating and plate reorganization: insights from numerical modelling and the NE Anatolia – Lesser Caucasus case example. J Geodyn 96: 35–49. https://doi.org/10.1016/j.jog.2016.02.007

Hussain E, Wright TJ, Walters RJ, Bekaert DPS, Lloyd R, Hooper A (2018) Constant strain accumulation rate between major earthquakes on the North Anatolian Fault. Nat Commun 9: 1392. https://doi.org/10.1038/s41467-018-03739-2

Jackson J (1994) Active tectonics of the Aegean region. Annu Rev Earth Planet Sci 22:239–271. https://doi.org/10.1146/annurev.ea.22.050194.001323

Joyner WB, Boore DM (1981) Peak horizontal acceleration and velocity from strong-motion records including records from the 1979 imperial valley California earthquake. Bull Seismol Soc Am 71:2011–2038

Kadirioğlu FT, Kartal RF (2016) The new empirical magnitude conversion relations using an improved earthquake catalogue for Turkey and its near vicinity (1900–2012). Turk J Earth Sci 25:300–310. https://doi.org/10.3906/yer-1511-7

Kadirioğlu FT et al (2016) An improved earthquake catalogue (M ≥ 4.0) for Turkey and its near vicinity (1900–2012). Bull Earthq Eng 16(8):3317–3338. 1-22. https://doi.org/10.1007/s10518-016-0064-8

Kalafat D, Güneş Y, Kekovali K, Kara M, Deniz P, Yilmazer M (2011) A revised and extended earthquake catalogue for Turkey since 1900 (M ≥ 4.0), Boğaziçi University, Kandilli Observatory and Earthquake Research Institute (KOERI), Bebek-Istanbul

Kale Ö, Akkar S (2013) A new procedure for selecting and ranking ground-motion prediction equations (GMPEs): the Euclidean distance-based ranking (EDR) method. Bull Seismol Soc Am 103:1069–1084. https://doi.org/10.1785/0120120134

Kelly D, Smith C (2011) Bayesian inference for probabilistic risk assessment: a practitioner's guidebook. Springer Science & Business Media,

Koçyiğit A, Yilmaz A, Adamia S, Kuloshvili S (2001) Neotectonics of East Anatolian Plateau (Turkey) and Lesser Caucasus: implication for transition from thrusting to strike-slip faulting. Geodin Acta 14:177–195. https://doi.org/10.1080/09853111.2001.11432443

Konca AO (2015) Rupture process of 2011 Mw7.1 Van, Eastern Turkey earthquake from joint inversion of strong-motion, high-rate GPS, teleseismic, and GPS data. J Seismol 19: 969–988. https://doi.org/10.1007/s10950-015-9506-z

Leptokaropoulos KM, Karakostas VG, Papadimitriou EE, Adamaki AK, Tan O, İnan S (2013) A homogeneous earthquake catalog for Western Turkey and magnitude of completeness determination. Bull Seismol Soc Am 103:2739–2751. https://doi.org/10.1785/0120120174

Lyubushin AA, Parvez IA (2010) Map of seismic hazard of India using Bayesian approach. Nat Hazards 55:543–556. https://doi.org/10.1007/s11069-010-9546-1

Lyubushin AA, Tsapanos TM, Pisarenko VF, Koravos GC (2002) Seismic hazard for selected sites in Greece: a Bayesian estimate of seismic peak ground acceleration. Nat Hazards 25: 83–98. https://doi.org/10.1023/a:1013342918801

McClusky S et al (2000) Global Positioning System constraints on plate kinematics and dynamics in the eastern Mediterranean and Caucasus. J Geophys Res Solid Earth 105:5695–5719. https://doi.org/10.1029/1999JB900351

McCuen RH, Knight Z, Cutter AG (2006) Evaluation of the Nash–Sutcliffe Efficiency Index 11:597-602 https://doi.org/10.1061/(ASCE)1084-0699(2006)11:6(597)

McGuire RK (2004) Seismic hazard and risk analysis. Earthquake Engineering Research Institute,

McKenzie D (1972) Active tectonics of the Mediterranean region. Geophys J R Astron Soc 30:109–185. https://doi.org/10.1111/j.1365-246X.1972.tb02351.x

McKenzie D (1976) The East Anatolian Fault: a major structure in Eastern Turkey. Earth Planet Sci Lett 29:189–193. https://doi.org/10.1016/0012-821X(76)90038-8

Megawati K, Pan T-C (2010) Ground-motion attenuation relationship for the Sumatran megathrust earthquakes. Earthq Eng Struct Dyn 39:827–845. https://doi.org/10.1002/eqe.967

Mohammadi H, Türker T, Bayrak Y (2016) A quantitative appraisal of earthquake hazard parameters evaluated from Bayesian approach for different regions in Iranian Plateau. Pure Appl Geophys 173:1971–1991. https://doi.org/10.1007/s00024-016-1264-5

Mortgat CP, Shah HC (1979) A Bayesian model for seismic hazard mapping. Bull Seismol Soc Am 69:1237–1251

Nas M, Jalilian A, Bayrak Y (2019) Spatiotemporal comparison of declustered catalogs of earthquakes in Turkey. Pure Appl Geophys 176:2215–2233. https://doi.org/10.1007/s00024-018-2081-9

Nash JE, Sutcliffe JV (1970) River flow forecasting through conceptual models part I — a discussion of principles. J Hydrol 10:282–290. https://doi.org/10.1016/0022-1694(70)90255-6

Pichon XL, Kreemer C (2010) The Miocene-to-present kinematic evolution of the Eastern Mediterranean and Middle East and its implications for dynamics. Annu Rev Earth Planet Sci 38:

323–351. https://doi.org/10.1146/annurev-earth-040809-152419

Pisarenko V, Lyubushin A (1999) A Bayesian approach to seismic hazard estimation: maximum values of magnitudes and peak ground accelerations. Earthq Res China 45–57

Pisarenko VF, Lyubushin AA (1997) Statistical estimation of maximum peak ground acceleration at a given point of a seismic region. J Seismol 1:395–405. https://doi.org/10.1023/a:1009795503733

Pisarenko VF, Lyubushin AA, Lysenko VB, Golubeva TV (1996) Statistical estimation of seismic hazard parameters: maximum possible magnitude and related parameters. Bull Seismol Soc Am 86:691–700

Rao CR (1965) Linear statistical inference and its applications. John Wiley & Sons,

Reilinger R et al. (2006) GPS constraints on continental deformation in the Africa-Arabia-Eurasia continental collision zone and implications for the dynamics of plate interactions. J Geophys Res: Solid Earth 111. https://doi.org/10.1029/2005JB004051

Reilinger RE et al (1997) Global Positioning System measurements of present-day crustal movements in the Arabia-Africa-Eurasia plate collision zone. J Geophys Res Solid Earth 102:9983–9999. https://doi.org/10.1029/96JB03736

Rong Y, Mahdyiar M, Shen-Tu B, Shabestari K (2011) Magnitude problems in historical earthquake catalogues and their impact on seismic hazard assessment. Geophys J Int 187:1687–1698. https://doi.org/10.1111/j.1365-246X.2011.05226.x

Royden LH (1993) Evolution of retreating subduction boundaries formed during continental collision. Tectonics 12:629–638. https://doi.org/10.1029/92TC02641

Ruzhich VV, Levina EA, Pisarenko VF, Lyubushin AA (1998) Statistic estimation of the maximum possible earthquake magnitude for the Baikal Rift Zone. Geol Geofiz 39:1445–1457

Salahshoor H, Lyubushin A, Shabani E, Kazemian J (2018) Comparison of Bayesian estimates of peak ground acceleration (Amax) with PSHA in Iran. J Seismol 22:1515–1527. https://doi.org/10.1007/s10950-018-9782-5

Saroglu F, Emre O, Kuscu I (1992) The East Anatolian Fault Zone of Turkey. Annales Tectonicae 6:99–125

Scherbaum F, Bommer JJ, Bungum H, Cotton F, Abrahamson NA (2005) Composite ground-motion models and logic trees: methodology, sensitivities, and uncertainties. Bull Seismol Soc Am 95:1575–1593. https://doi.org/10.1785/0120040229

Scherbaum F, Cotton F, Smit P (2004) On the use of response spectral-reference data for the selection and ranking of ground-motion models for seismic-hazard analysis in regions of moderate seismicity: the case of rock motion. Bull Seismol Soc Am 94:2164–2185. https://doi.org/10.1785/0120030147

Scherbaum F, Delavaud E, Riggelsen C (2009) Model selection in seismic hazard analysis: an information-theoretic perspective. Bull Seismol Soc Am 99:3234–3247. https://doi.org/10.1785/0120080347

Scherbaum F, Kuehn NM (2011) Logic tree branch weights and probabilities: summing up to one is not enough. Earthquake Spectra 27:1237–1251. https://doi.org/10.1193/1.3652744

Şengör AMC, Yilmaz Y (1981) Tethyan evolution of Turkey: a plate tectonic approach. Tectonophysics 75:181–241. https://doi.org/10.1016/0040-1951(81)90275-4

Şengör AMC, Görür N, Şaroğlu F (eds) (1985) Strike-slip faulting and related basin formation in zones of tectonic escape: Turkey as a case study vol 37. Strike-slip deformation, basin formation, and sedimentation Society of Economic Paleontologists and Mineralogists Special Publication,

Shebalin NV, Leydecker G, Mokrushina NG, Tatevossian RE, Erteleva OO, Vassiliev Y-V (1998) Earthquake catalogue for central and southeastern Europe 342 BC - 1990 AD. Commission of the European Union, Brussels

Softa M, Emre T, Sözbilir H, Spencer JQG, Turan M (2018) Geomorphic evidence for active tectonic deformation in the coastal part of Eastern Black Sea, Eastern Pontides, Turkey. Geodin Acta 30:249–264. https://doi.org/10.1080/09853111.2018.1494776

Softa M, Emre T, Sözbilir H, Spencer JQG, Turan M (2019) Field evidence for Southeast Black Sea Fault of Quaternary age and its tectonic implications, Eastern Pontides, Turkey. Geol Bull Turkey 62:17–40

Sosson M et al (2016) The eastern Black Sea-Caucasus region during the Cretaceous: new evidence to constrain its tectonic evolution. Compt Rendus Geosci 348:23–32. https://doi.org/10.1016/j.crte.2015.11.002

Soysal H, Sipahioğlu S, Kolçak D, Altınok Y (1981) Historical earthquake catalogue of Turkey and surrounding area (2100 BC–1900 AD). Scientific and Technological Research Council of Turkey (TUBITAK), Istanbul, Turkey

Stucchi M et al (2013) The SHARE European Earthquake Catalogue (SHEEC) 1000–1899. J Seismol 17:523–544. https://doi.org/10.1007/s10950-012-9335-2

Şengör AMC (2014) Triple junction. In: Harff J, Meschede M, Petersen S, Thiede J (eds) Encyclopedia of marine geosciences. Springer Netherlands, Dordrecht, pp 1–13. https://doi.org/10.1007/978-94-007-6644-0_122-2

Şengör AMC, Tüysüz O, İmren C, Sakınç M, Eyidoğan H, Görür N, le Pichon X, Rangin C (2005) The North Anatolian Fault: a new look. Annu Rev Earth Planet Sci 33:37–112. https://doi.org/10.1146/annurev.earth.32.101802.120415

Şengör AMC, Yilmaz Y, Sungurlu O (1984) The geological evolution of the Eastern Mediterranean. Blackwell Scientific Publications, Palo Alto

Şeşetyan K, Demircioglu MB, Duman TY, Çan T, Tekin S, Azak TE, Fercan ÖZ (2018) A probabilistic seismic hazard assessment for the Turkish territory—part I: the area source model. Bull Earthq Eng 16:3367–3397. https://doi.org/10.1007/s10518-016-0005-6

Tan O, Tapirdamaz MC, Yörük A (2008) The earthquake catalogues for Turkey. Turk J Earth Sci 17:405–418

Tatar O, Akpınar Z, Gürsoy H, Piper JDA, Koçbulut F, Mesci BL, Polat A, Roberts AP (2013) Palaeomagnetic evidence for the neotectonic evolution of the Erzincan Basin, North Anatolian Fault Zone. Turkey Journal of Geodynamics 65:244–258. https://doi.org/10.1016/j.jog.2012.03.009

Tsapanos TM (2003) Appraisal of seismic hazard parameters for the seismic regions of the east circum-Pacific belt inferred from a Bayesian approach. Nat Hazards 30:59–78. https://doi.org/10.1023/a:1025051712052

Tsapanos TM, Christova CV (2003) Earthquake hazard parameters in Crete Island and its surrounding area inferred from Bayes statistics: an integration of morphology of the seismically active structures and seismological data. Pure Appl

Geophys 160:1517–1536. https://doi.org/10.1007/s00024-003-2358-4

Tsapanos TM, Lyubushin AA, Pisarenko VF (2001) Application of a Bayesian approach for estimation of seismic hazard parameters in some regions of the circum-pacific belt. Pure Appl Geophys 158:859–875

Turkelli N et al (2003) Seismogenic zones in Eastern. Turkey Geophys Res Lett 30:n/a. https://doi.org/10.1029/2003GL018023

Tuyen NH, Lu NT (2012) Recognition of earthquake-prone nodes, a case study for North Vietnam (M ≥ 5.0). Geodesy Geodyn 3:14–26. https://doi.org/10.3724/SP.J.1246.2012.00014

Utkucu M (2013) 23 October 2011 Van, Eastern Anatolia, earthquake (MW7.1) and seismotectonics of Lake Van area. J Seismol 17:783–805. https://doi.org/10.1007/s10950-012-9354-z

Vialon P, Ruhland M, Grolier J (1976) Eléments de tectonique analytique. Masson Paris

Westaway R (1994) Present-day kinematics of the Middle East and eastern Mediterranean. J Geophys Res Solid Earth 99:12071–12090. https://doi.org/10.1029/94jb00335

Wilcox RE, Harding TP, Seely DR (1973) Basic wrench tectonics. AAPG Bull 57:74–96

Yadav RBS, Tsapanos TM, Bayrak Y, Koravos GC (2013a) Probabilistic appraisal of earthquake hazard parameters deduced from a Bayesian approach in the northwest frontier of the Himalayas. Pure Appl Geophys 170:283–297. https://doi.org/10.1007/s00024-012-0488-2

Yadav RBS, Tsapanos TM, Tripathi JN, Chopra S (2013b) An evaluation of tsunami hazard using Bayesian approach in the Indian Ocean. Tectonophysics 593:172–182. https://doi.org/10.1016/j.tecto.2013.03.004

Yaghmaei-Sabegh S (2012) A new method for ranking and weighting of earthquake ground-motion prediction models. Soil Dyn Earthq Eng 39:78–87. https://doi.org/10.1016/j.soildyn.2012.03.006

Yılmaz Y, Tüysüz O, Yiğitbaş E, Genç ŞC, Şengör AMC (1997) Geology and tectonic evolution of the Pontides. In: Robinson AG (ed) Regional and petroleum geology of the Black Sea and surrounding regions, vol 68. The American Association of Petroleum Geologists Memoir, pp 183–226